Hydrophobicity of Model Surfaces with Loosely Packed Polystyrene Spheres after Plasma Etching

Liling Yan,[†] Ke Wang,[‡] Jingshen Wu,[§] and Lin Ye*[,†]

Centre for Advanced Materials Technology, School of Aerospace, Mechanical and Mechatronic Department, University of Sydney, Australia, NSW 2006, Molecular and Performance Materials Cluster, Institute of Materials Research and Engineering, 3 Research Link, Singapore, 117602, and Department of Mechanical Engineering, Hong Kong University of Science and Technology, Clear Water Bay, Kowloon, Hong Kong

Received: December 11, 2005; In Final Form: March 31, 2006

Polystyrene (PS) sphere films with loosely packed arrays were prepared by plasma etching of closely packed PS sphere arrays. The size of PS spheres can be efficiently reduced with plasma etching, and surface topography can be manipulated by controlling the initial PS sphere size and the time of plasma exposure. These surfaces with loosely packed arrays provide a well-characterized model system for studying water repellency behavior. It was found that the surface hydrophobicity could be systematically tailored due to the well-defined and controlled surface topography. Sphere size and the interparticle distance between two adjacent spheres are critical factors in determining the water repellency behavior of the surface. A model based on the Cassie theory was proposed to elucidate the effect of surface topography on hydrophobicity, and the predicted contact angles agree well with the experimental results.

1. Introduction

It is well-known that surface topographic geometry is a decisive factor in determining surface wettability or hydrophobicity.[1−4] Many surfaces with a superhydrophobic property, that is, with a water contact angle of more than 150°, have been successfully developed by introducing appropriate roughness on materials with low surface energy.[5−11]

Model surfaces consisting of nano- or microspheres are of special interest because they resemble the characteristics of many real superhydrophobic surfaces.[11−14] In a recent study,[15] Shiu et al. prepared surfaces with loosely packed polystyrene (PS) arrays fabricated by treating closely packed arrays of PS spheres of 440 nm in diameter with oxygen plasma. It was shown that the contact angle increased significantly with a reduction in sphere size. In that study, however, there was no discussion of the effects of other variables such as interparticle distance. Only one initial sphere size, 440 nm, was studied.

In our previous study,[16] the hydrophobicity of surfaces with closely packed sphere arrays of different sizes (from nano- to microscale) was reported. It was found that the contact angle value for closely packed structures is almost constant, independent of sphere size. In the present study, loosely packed PS arrays were prepared with plasma etching over the closely packed PS array to further improve hydrophobicity.

The process of plasma etching has proven to be an effective way of accurately regulating particle size.[17,18] After plasma etching, the diameters of PS spheres are reduced and intersphere space is introduced between spheres, which is dependent on the amount of removed substances. With the plasma technique, sphere size can be controlled by adjusting the plasma reaction conditions, while the interparticle distance (defined as the distance between the centers of adjacent spheres) can also be controlled by selecting the initial size of the polystyrene spheres. In such a way, films with a fixed interparticle distance but different sphere sizes or films with a fixed sphere size but different interparticle distances can be produced, as shown in Figure 1. The surface topography is therefore described in terms of sphere size and interparticle distance. Thus, the effects of sphere size and interparticle distance on surface hydrophobicity can be systematically elaborated.

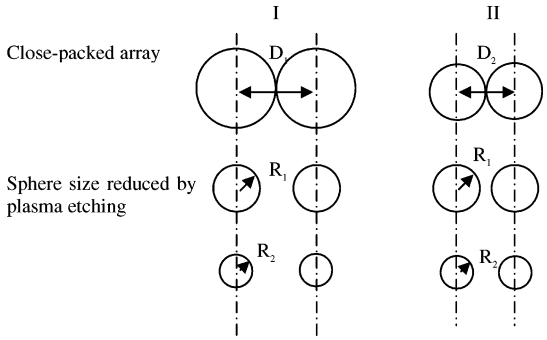

Figure 1. Methodology for obtaining surfaces with loosely packed spheres with reduced sphere size and interparticle distance being controllable. Columns I and II represent different initial sphere sizes, i.e., different interparticle distances.

2. Experimental Section

2.1. Materials. Micro- and nano-PS spheres in the form of an aqueous suspension were purchased from Polysciences, Inc. Spheres with diameters of 200 nm (size distribution, S.D. = 8%), 300 nm (S.D. = 8%), 500 nm (S.D. = 3%), 1000 nm (S.D. = 3%), and 2000 nm (S.D. = 5%) were used. All of the as-received colloids had a solid concentration of 2.6 wt %.

Normal cover glasses (18 mm × 18 mm) for an optical microscope were used as substrates, cleaned by immersing them in H_2SO_4/H_2O_2 (7:3 v/v, piranic acid) for 30 min, followed by

* To whom correspondence should be addressed. Phone: (+61) 02-93514798. Fax: (+61) 02-93517060. E-mail: ye@aeromech.usyd.edu.au.
[†] University of Sydney.
[‡] Institute of Materials Research and Engineering.
[§] Hong Kong University of Science and Technology.

10.1021/jp057228z CCC: $33.50
Published on Web 05/19/2006

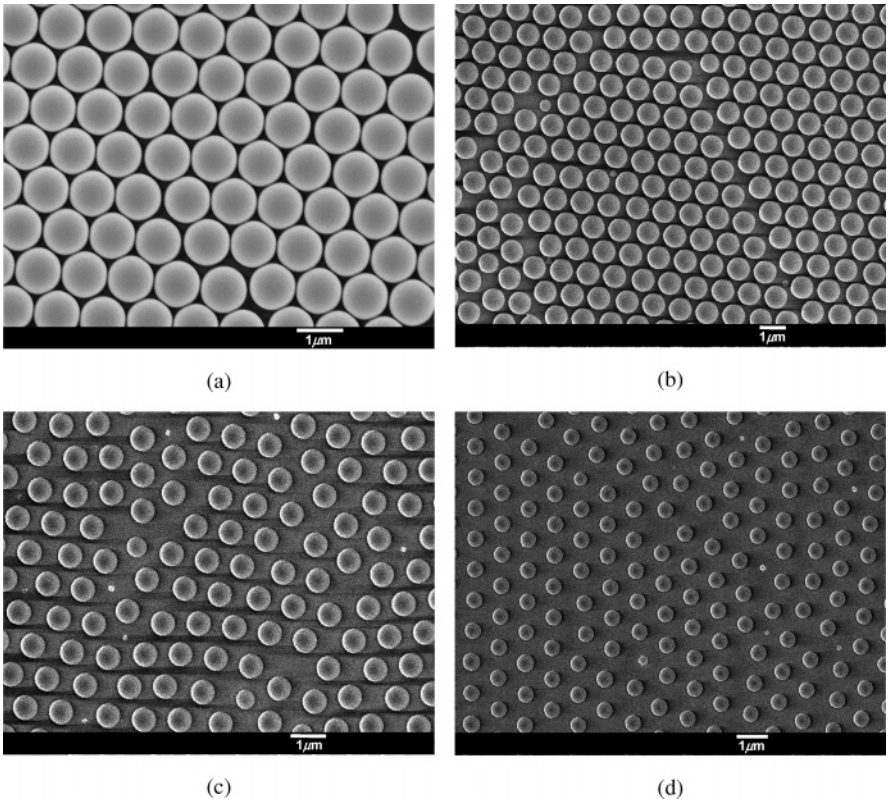

Figure 2. SEM images of PS sphere films. (a) Initial 1000 nm spheres in closely packed array and thinned PS spheres in loosely packed arrays: (b) 845 nm; (c) 687 nm; (d) 530 nm.

rinsing with copious deionized water. A water drop deposited on the cleaned dry glass surface becomes a thin film and has a contact angle of nearly 0°. The substrates were then preserved in deionized water before use.

A flat PS plate was prepared as a reference for PS films and was compression-molded at 180 °C by sandwiching PS pellets (Polystyrol 147F, BASF) between two pieces of tempered glass plate.

2.2. Film Preparation. Single-layer films of PS spheres were formed by means of angle sedimentation.[19] The PS suspension was diluted with ethanol to 1 wt %. A droplet of diluted solution was deposited on a precleaned glass plate placed at a tilt angle of 10°. The whole system was covered with a crystallizing dish to avoid external disturbance. The temperature for this process was set to 23 °C with ±1 °C deviation.

2.3. Plasma Etching. The films of PS spheres were etched in a plasma reactor (JEH-OOTS, JEOL) with argon (99.998%) as a process gas. The specimens with closely packed sphere arrays were inserted into the circular reactor chamber which was then evacuated to ∼0.07 mmHg. Argon was introduced using a needle valve, and the pressure was equilibrated to 0.5 mmHg by adjusting the valve. Radio frequency (rf) power at 60 W was applied after equilibrium pressure was reached. The flow rate was measured to be ∼1.4 sccm. After the plasma treatment, most films were subjected to an annealing treatment in an oven at 76 °C for 24 h. This process tends to moderate the surface roughness of PS spheres caused by plasma processing, and its function will be elaborated later.

2.4. Surface Chemistry Modification. All of the prepared films were chemically modified by a fluoroalkylsilane (tridecafluorooctyltriethoxysilane, $CF_3(CF_2)_5(CH_2)_2Si(OCH_2CH_3)_3$, DYNASYLAN F8261, Degussa Chemicals Pte Ltd) in order to render the surface hydrophobicity. The silane was used without further purification. To deposit the silane onto the film surfaces, the specimens were placed together into a Teflon container with an aluminum cup filled with 0.2 mL of silane. The container was sealed and placed in an oven maintained at 65 °C for 5 h. The same modification procedure was also applied to the reference PS flat plate.

2.5. Characterization. The morphology of the etched film surfaces of PS spheres was investigated using field emission scanning electron microscopy (FEG-SEM, JEOL 6700F). A thin layer of gold was sputtered onto all specimens prior to imaging, to improve conductivity.

The wettability of the surfaces was characterized by contact angle measurement using sessile water droplets. Using a goniometer (Ramé-Hart 100-series) with an automatic dispensing system, the contact angle image was acquired by dispensing a 5 μL sized deionized water drop. The accuracy of this instrument is of the order of ±1°. At least 10 measurements were averaged for all of the data reported here. All of the measurements were performed at room temperature.

3. Results and Discussion

3.1. Morphology. The morphology of closely packed PS sphere arrays has been reported in our previous study.[16] Figure 2 shows SEM images of PS sphere arrays before and after plasma treatment and annealing. The initial PS sphere size shown here is 1000 nm. The sphere size was effectively reduced by plasma etching, while the distance between the centers of adjacent spheres was a constant given by the initial sphere diameter, that is, 1000 nm. Because the plasma acted onto the sphere surface is nondirectional in the circular reactor, the entire sphere surface was exposed to plasma except for the area contacting with the substrate. Thus, the PS spheres were almost uniformly etched and the final product remains nearly a spherical shape. The same phenomenon has been reported by Shiu et al.[15] and Haginoya et al.[18]

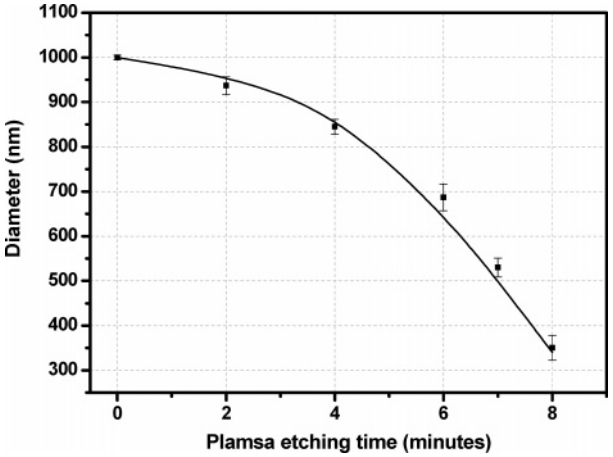

Figure 3. Relation between plasma etching time and the diameter of reduced polystyrene spheres.

Particle size can be systematically controlled by the etching process. The relationship between etching time and the diameter of reduced particles is presented in Figure 3. Using plasma etching, patterned surfaces with spheres of any diameter can be obtained by controlling the etching time. In this way, various sizes of PS spheres in desirable arrays were manufactured by choosing an appropriate initial diameter of PS spheres.

An interesting phenomenon was noticed in the plasma etching. Besides reducing the polymer sphere size, plasma bombardment also induces roughness on the PS sphere surface. The effect of surface roughness induced by plasma etching has been widely recognized.[20] Figure 4a shows the freshly etched surface of PS spheres of 530 nm reduced from 1000 nm. Although the initial spherical surface is smooth and clean (Figure 2a), nanoscale spikes appeared on the spherical surface after the plasma etching. The surface roughness was more obvious for films etched for a longer time than for shorter duration etching, although the overall spherical shape was not affected. The surface roughening is attributable to plasma microscopically inhomogeneous etching.[15,18]

To remove such roughness on sphere surfaces caused by plasma, the etching process was followed by an annealing treatment. The annealing temperature was controlled at 76 °C, which is slightly lower than the glass transition temperature of PS (i.e., T_g = 80 °C, provided by the PS microsphere manufacturer). The films were annealed at this temperature because polymer chain mobility at regimes near T_g facilitates the minimization of the surface area of polystyrene particles by eliminating the spikes. One day's annealing effectively removed the surface roughness, and the etched sphere surface became smooth again, as shown in Figure 4b.

TABLE 1: Effect of Multiscale Roughness on Water Contact Angles (deg)

reduced sphere size (nm)	multiscale-roughness structure (fresh plasma-etched samples)	single-scale roughness structure (annealed samples)
770	130 ± 2	130 ± 1
530	135 ± 1	135 ± 2

3.2. Hydrophobicity of Various Films. Although plasma etching caused some roughness on the sphere surface, such a hierarchically structured surface may be very helpful in identifying the effects of multiscale roughness on water repellency behavior. There has been argument that multiscale roughness or hierarchical roughness is the main factor in rendering surfaces superhydrophobic; that is, it can enhance hydrophobicity more than single-scale roughness.[21−23]

To elaborate this argument in the present system, water contact angles of both the freshly plasma-etched and the annealed films were measured. The results of two sets of films with reduced sphere sizes of 770 and 530 nm, respectively, are listed in Table 1. Note that the diameter of the initial sphere size is 1000 nm. It was found that the water contact angles of both the freshly etched and the annealed films were identical within the limits of experimental error. It seems, then, that the nanoscale roughness on the sphere surface induced by plasma reaction has no significant influence on the apparent hydrophobicity of the surface.

In fact, most multiscale rough superhydrophobic surfaces display a much greater roughness scale than present surfaces. For instance, the lotus surface has protrusions as large as ~20 μm, and the fine microtexture on the protrusions is as small as 200 nm−1 μm.[11] Theoretical analysis[23] by Patankar indicates that multiscale roughness (both coarse and fine microtexture) must satisfy a certain condition for the fine scale roughness to play a significant role in hydrophobicity. The coarse roughness in the present system is less than 2 μm, and the fine roughness is in a scale of several nanometers only. It is believed that such a fine roughness scale is not sufficient enough to have an impact on a macroscopic property, that is, the water contact angle. Coincidentally, Shiu et al.[15] also found that the fine structure caused by plasma etching was not important in the water repellency behavior of surfaces consisting of microspheres.

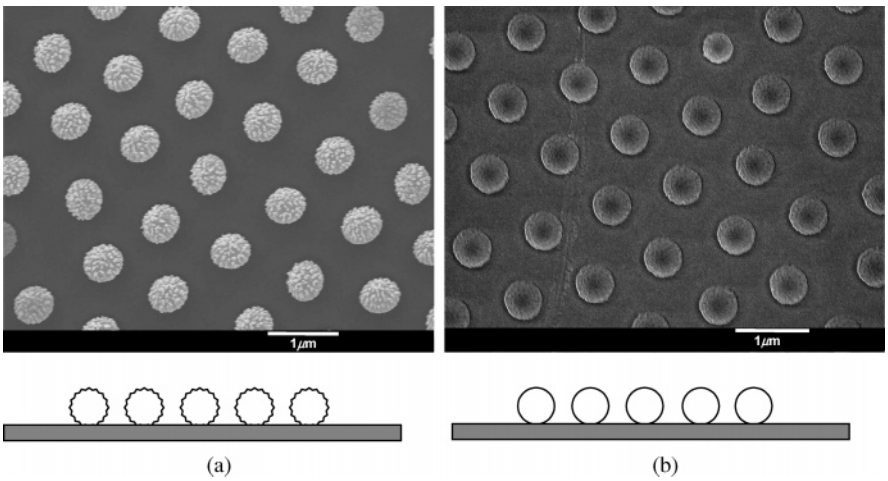

Figure 4. SEM images of PS sphere films reduced from 1000 to 530 nm: (a) freshly plasma-treated film; (b) annealed film. The figures under each SEM image are schematic views of individual spheres.

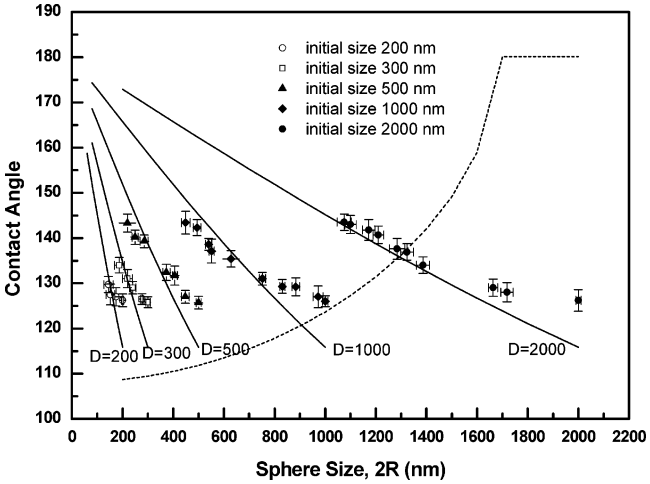

Figure 5. Apparent water contact angle versus PS sphere size with solid lines for the Cassie contact angles and a dotted line for the Wenzel contact angle.

A series of contact angle data were obtained for PS sphere films with initial sphere sizes ranging from 200 to 2000 nm. Figure 5 shows the relationship between contact angle and reduced sphere size, with scattered dots as experimental data. It is observed that the water contact angle increases as the sphere size reduces. For instance, the contact angle of PS film with closely packed 500 nm PS spheres is 126°.[16] When the diameter of PS spheres was reduced to 373 nm by argon plasma treatment, the contact angle of the modified surface increased to 132°. With a further size reduction to 219 nm, the contact angle increased to 143°. This phenomenon of hydrophobicity increasing with the reduction of sphere size was utilized to fabricate superhydrophobic surfaces by Shiu et al.[15]

It also can be seen that, given the same reduced sphere size, PS films with a large interparticle distance are more hydrophobic than those with a small interparticle distance. Furthermore, Figure 5 also reveals the sensitivity of hydrophobicity due to the change of sphere size. The slope varies for each set of films; that is, the smaller the initial sphere size, the steeper the slope, and vice versa. For example, the slope of the modified 1000 nm films is higher than that of the 2000 nm counterparts and lower than that of the 500 nm films. In addition, the results in Figure 5 confirm that in general reduced sphere size has a more positive impact on hydrophobicity when the interparticle distance is small.

Takeshita et al.[24] reported that surfaces containing 100 nm particles were not as hydrophobic as surfaces with 350 nm spheres, and the surface coverage (34 and 48%, respectively) did not affect the surface hydrophobicity. These results seem contradictory to observations in the present study, but the disagreement may be attributed to the fact that the spheres in Takeshita's system were randomly scattered, unlike the periodic arrays in the present system. Randomness and irregularity probably limit investigation of the effects of variables such as sphere size, interparticle distance, and surface coverage.

3.3. Modeling of Hydrophobicity. There are two well-acknowledged theories describing the water repellency behavior of rough hydrophobic surfaces, Wenzel theory[25] and Cassie–Baxter theory,[26] which are mathematically expressed by eqs 1 and 2, respectively.

$$\cos \theta_r^w = r_w \cos \theta_0 \tag{1}$$

$$\cos_r^c = \phi_s \cos \theta_0 + \phi_s - 1 \tag{2}$$

Wenzel theory assumes that the liquid droplet is completely in contact with the surface over their mutual interface, wetting even the grooves of the rough surface. Such a contact mode is often referred to as the Wenzel contact mode. In contrast, Cassie theory assumes that the liquid droplet sits on top of peaks of the rough surface, leaving air trapped in surface grooves. Similarly, the Cassie contact mode is used to refer to this wetting behavior.

However, both theories need to be modified for application to specific circumstances.[27−29] In the current system, the surface is characterized in terms of sphere size and interparticle distance, based on which the correlations between the surface geometric parameters and contact angle can be established.

A model surface, proposed by Fabretto et al.,[30] can be considered as a general case of the present system. It consists of a number of randomly scattered cylinders capped with hemispheres. The Wenzel roughness ratio of the model is given by[30]

$$r_w = 1 + \frac{3\pi}{4} d^2 n \tag{3}$$

where n is the number concentration of particles in area A_0 and is given by $n = N_F/A_0$, N_F is the total number of particles in area A_0, and d is the diameter of hemispheres.

The number concentration, n, is a constant for each set of modified PS films in the present system, being determined by the initial closely packed configuration, regardless of the final reduced sphere sizes. For each set of modified films, the roughness, r_w, is a function of the diameter of hemispheres or spheres, d, only. Equation 3 indicates that r_w decreases when the sphere size decreases. Thus, the contact angle given by the Wenzel equation is

$$\cos \theta_r^w = \left(1 + \frac{3\pi}{4} d^2 n\right) \cos \theta_0 \tag{4}$$

Equation 4 suggests that the Wenzel contact angle decreases when the sphere size decreases, which, however, is apparently contradictory to the present observations.

A more vigorous analysis with the Wenzel approach on a model system with a loosely packed array rather than a random irregular arrangement is necessary to further elaborate whether the Wenzel theory is applicable to the current system. Figure 6a schematically shows the surface with spheres in a loosely packed array. Suppose there are N spheres in a unit length, D is the distance between the centers of adjacent spheres, and R is the radius of the spheres. Then, the real surface area includes two parts, that is, the projected area without spheres and the protruded area caused by the peripheral surface of spheres. Therefore, the total surface is expressed by

$$A_r = (N-1)^2 D^2 + N^2 4\pi R^2 \tag{5}$$

Then, the Wenzel roughness factor, r_w, determined by the ratio of the real surface area, A_r, and the projected area, A_0, is

$$r_w = \frac{A_r}{A_0} = \frac{(N-1)^2 D^2 + N^2 4\pi R^2}{(N-1)^2 D^2} = 1 + \frac{4\pi R^2}{D^2} \tag{6}$$

Substituting eq 6 into eq 1, the Wenzel contact angle thus can be calculated by

$$\cos \theta_r^w = \left(1 + \frac{4\pi R^2}{D^2}\right) \cos \theta_0 \tag{7}$$

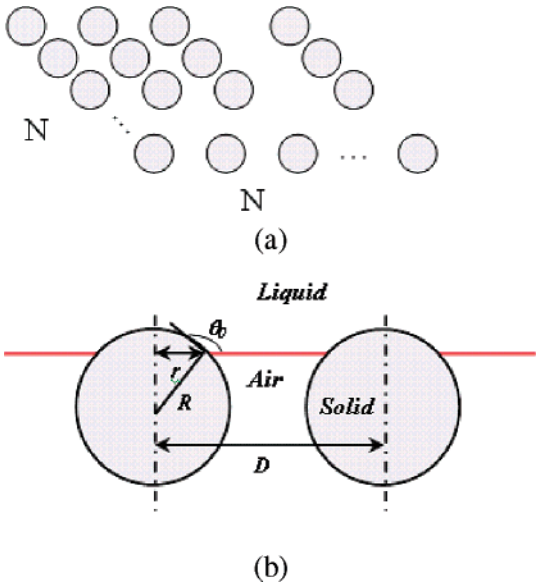

Figure 6. Schematic of a liquid drop sitting on a number of spheres in a loosely packed array: (a) view from above; (b) side view.

Equation 7 suggests again that when D is a constant, reducing the sphere size, R, leads to a smaller r_w value and consequently results in a smaller contact angle if the Wenzel equation applies.

Obviously, the predicted Wenzel contact angle disagrees with the experimental results. The Cassie theory, therefore, is considered to model the current system. For Cassie theory, it is necessary to know the area fraction above the liquid−solid contact line. Assuming the water contact line lies on the upper part of spheres (Figure 6b), the liquid−solid contact area is determined by

$$A_s = 2\pi R^2[1 - \cos(\pi - \theta_0)]N^2 \quad (8)$$

The total projected area under the water droplet is given by

$$A_p = (N-1)^2 D^2 \quad (9)$$

Then, the liquid−air contact area is given by

$$A_{air} = A_p - N^2\pi r^2 \quad (10)$$

where r is the radius of the sphere cap embedded in the water droplet and is given by $r = R \sin\theta$. Therefore, the solid−liquid contact area fraction, ϕ_s, is given by

$$\phi_s = \frac{A_s}{A_s + A_{air}} = \frac{2\pi R^2(1+\cos\theta_0)}{D_2 - \pi R^2 \sin^2\theta_0 + 2\pi R^2(1+\cos\theta_0)} \quad (11)$$

Substituting eq 11 into eq 2, the Cassie contact angle is thus explicitly given by

$$\cos\theta_r^c = \frac{2\pi R^2(1+\cos\theta_0)^2}{D_2 - \pi R^2 \sin^2\theta_0 + 2\pi R^2(1+\cos\theta_0)} - 1 \quad (12)$$

Equation 12 is referred to as the "modified" Cassie equation. The contact angles predicted by the equation are plotted in Figure 5 (shown as solid lines) for different interparticle distances as a function of reduced sphere size and distance between sphere centers. The theoretical results agree well with the experimental data, revealing that the modified Cassie model is successful in describing the water repellency behavior of the surfaces consisting of spheres in a loosely packed structure. For comparison, the five solid lines in Figure 5 represent the calculated contact angles versus the reduced sphere sizes using the modified Cassie equation, each of which is for a different interparticle distance, while the dotted line represents the Wenzel contact angle with the reduced diameters for the case of 2000 nm modified films.

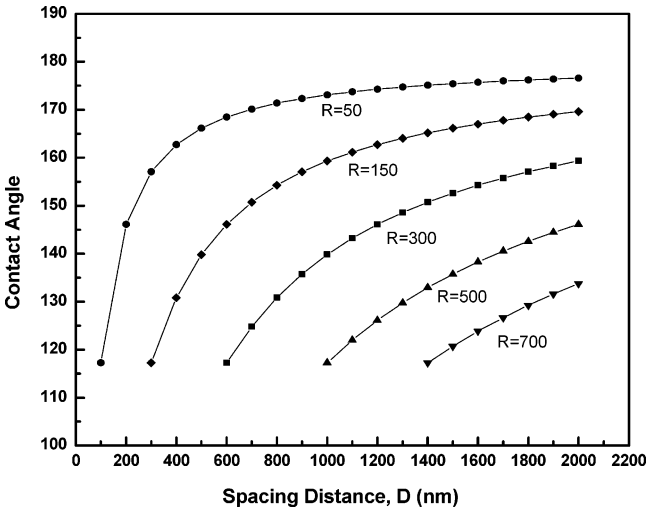

Figure 7. Apparent water contact angle versus interparticle distance. Each curve represents a different sphere size.

It is interesting to note that the solid−liquid fraction area, ϕ_s, is also a function of interparticle distance, D, as indicated in eq 11. It decreases as the interparticle distance increases, leading to an increase in the contact angle, which again agrees with the experimental observations. The trend of contact angle versus interparticle distance is more straightforwardly illustrated in Figure 7.

From this discussion, it seems that an extreme contact angle (i.e., 180°) could be obtained by further reducing the sphere size. However, if the sphere size is equal to zero, it is expected that the contact angle should be equal to θ_0, since the surface is an ideally flat surface. This contradiction is due to the transition of the contact mode. When the sphere size approaches zero, the liquid above the spheres probably intrudes into cavities between the spheres. The water droplets tend to wet the whole area underneath, that is, the Wenzel contact mode, instead of standing on the air cushion between spheres, that is, the Cassie contact mode. Hence, in this extreme case, eq 12 derived from Cassie equation is not valid.

4. Conclusions

Loosely packed single-layer PS sphere surfaces with spheres of different diameters in the nanoscale were effectively produced from initially closely packed PS sphere films using plasma etching. The final sphere size and interparticle distance can be accurately controlled by selecting the initial sphere size and etching time. Study of the surface hydrophobicity of the model surfaces constructed with loosely packed spheres revealed that the contact angle is a function of sphere size and interparticle distance. The results show that the contact angle increases as the sphere size decreases when the interparticle distance is constant, whereas it decreases as the interparticle distance decreases when the sphere size is constant. The experimental observations can be well explained using a modified Cassie equation that specifically addresses the water contact angle on surfaces with spherical protrusions. The prediction correlates well with experimental data.

Acknowledgment. We thank the Australian Department of Education, Science and Training (DEST) and the University of Sydney for financial support. We acknowledge the use of the MCPF central facilities at HKUST. L.Y. would like to express her gratitude to Degussa Chemicals Pte Ltd for providing the silane.

References and Notes

(1) Bikerman, J. J. *J. Phys. Colloid Chem.* **1950**, *54*, 653.
(2) Johnson, R. E., Jr.; Dettre, R. H. *Adv. Chem. Ser.* **1964**, *43*, 112.
(3) Hazlett, R. D. *J. Colloid Interface Sci.* **1990**, *137*, 527.
(4) Chow, T. S. *J. Phys.: Condens. Matter* **199**8, *10* (27), L445.
(5) Onda, T.; Shibuichi, S.; Satoh, N.; Tsujii, K. *Langmuir* **1996**, *12*, 2125.
(6) Nakajima, A.; Fujishima, A.; Hashimoto, K.; Watanabe, T. *Adv. Mater.* **1999**, *11*, 1365.
(7) Morra, M.; Occhiello, E.; Garbassi, F. *Langmuir* **1989**, *5*, 872.
(8) Yamauchi, G.; Miller, J. D.; Saito, H.; Takai, K.; Ueda, T.; Takazawa, H.; Yamamoto, H.; Nislhi, S. *Colloids. Surf., A* **1996**, *116*, 125.
(9) Chen, W.; Fadeev, A. Y.; Hsieh, M. C.; Oner, D.; Youngblood, J.; McCarthy, J. *Langmuir* **1999**, *15*, 3395.
(10) Shibuichi, S.; Onda, T.; Satoh, N.; Tsujii, K. *J. Phys. Chem.* **1996**, *100*, 19512.
(11) Barthlott, W.; Neinhuis, C. *Planta* **1997**, *202*, 1.
(12) Teare, D. O. H.; Spanos, C. G.; Ridley, P.; Kinmond, E. J.; Roucoules, V.; Coulson, S.; Brewer, S. A.; Willis, C.; Badyal, J. P. S. *Chem. Mater.* **2002**, *14*, 4566.
(13) Erbil, H. Y.; Demirel, A. L.; Avci, Y.; Mert, O. *Science* **2003**, *299* (5611), 1377.
(14) Yan, L. L.; Wang, K.; Ye, L. *J. Mater. Sci. Lett.* **2003**, *22*, 1713.
(15) Shiu, J. Y.; Kuo, C. W.; Chen, P. L.; Mou, C. Y. *Chem. Mater.* **2004**, *16*, 561.
(16) Yan, L.; Wang, K.; Wu, J. S.; Ye, L. *Colloids Surf., A.*, submitted for publication.
(17) Stoffels, W. W.; Stoffels E.; Swinkels, G. H. P. M.; Boufnichel, M.; Krosesen, G. M. W. *Phys. Rev. E* **1999**, *59*, 2302.
(18) Haginoya, C.; Ishibashi, M.; Koike, K. *Appl. Phys. Lett.* **1997**, *71*, 2934.
(19) Micheletto, R.; Fukuda, H.; Ohtsu, M. *Langmuir* **1995**, *11*, 3333.
(20) Zhao, Y. P.; Drotar J. T.; Wang G. C.; Lu, T. M. *Phys. Rev. Lett.* **1999**, *82*, 4882.
(21) Herminghaus, S. *Europhys. Lett.* **2000**, *52*, 165.
(22) Otten, A.; Herminghaus, S. *Langmuir* **2004**, *20*, 2405.
(23) Patankar, N. A. *Langmuir* **2004**, *20*, 8209.
(24) Takeshita, N.; Paradis, L. A.; Oner, D.; McCarthy, T. J.; Chen, W. *Langmuir* **2004**, *20*, 8131.
(25) Wenzel, R. N. *Ind. Eng. Chem.* **1936**, *28*, 988.
(26) Cassie, A. B. D.; Baxter, S. *Trans. Faraday Soc.* **1944**, *40*, 546.
(27) Bico, J.; Marzolin, C.; Quere, D. *Europhys. Lett.* **1999**, *47*, 220.
(28) Patankar, N. A. *Langmuir* **2003**, *19*, 1249.
(29) Marmur, A. *Langmuir* **2003**, *19*, 8343.
(30) Fabretto, M.; Sedev, R.; Ralson, J. In *Contact Angle, Wettability and Adhesion*; Mittal, K. L., Ed.; VSP: Utrecht, The Netherlands, 2003; Vol. 3, pp 161−173.